DOI: 10.1002/chem.200601051

Experimental and DFT Study of the Tautomeric Behavior of Cobalt-Containing Secondary Phosphine Oxides

Chu-Hung Wei, Cheng-En Wu, Yi-Luen Huang, Roman G. Kultyshev, and Fung-E. Hong*[a]

Abstract: New cobalt-containing secondary phosphine oxides [(μ-$PPh_2CH_2PPh_2$)$Co_2(CO)_4${μ,η-PhC≡C-P(=O)(H)(R)}] (**8a**: R = *t*Bu; **8b**: R = Ph) were prepared by reaction of secondary phosphine oxides PhC≡CP-(=O)(H)(R) (**6a**: R = *t*Bu; **6b**: R = Ph) with dppm-bridged dicobalt complex [(μ-$PPh_2CH_2PPh_2$)$Co_2(CO)_6$] (**2**). The molecular structures of **8a** and **8b** were determined by single-crystal X-ray diffraction. Although palladium-catalyzed Heck reactions employing **8b** as ligand gave satisfying results, **8a** performed poorly in the same reaction. Judging from these results, a tautomeric equilibrium between **8b** and its isomeric form [(μ-$PPh_2CH_2PPh_2$)$Co_2(CO)_4${μ,η-PhC≡CP(OH)(Ph)}] **8b′** indeed takes place, but it is unlikely between **8a** and [(μ-$PPh_2CH_2PPh_2$)$Co_2(CO)_4${μ,η-PhC≡CP(OH)(*t*Bu)}] (**8a′**). The DFT studies demonstrated that reasonable activation energies for the tautomeric conversions can be achieved only via a bimolecular pathway. Since a *t*Bu group is much larger than a Ph group, the conversion is presumably only feasible in the case of **8b**⇌**8b′**, but not in the case of **8a**⇌**8a′**. Another cobalt-containing phosphine, namely, [(μ-$PPh_2CH_2PPh_2$)$Co_2(CO)_4${μ,η-PhC≡CP-(NEt$_2$)(*t*Bu)}] (**7a**), and its oxidation product [(μ-$PPh_2CH_2PPh_2$)$Co_2(CO)_4$-{μ,η-PhC≡CP(=O)(NEt$_2$)(*t*Bu)}] **7a′** were prepared from the reaction of PhC≡CP(NEt$_2$)(*t*Bu) (**5a**) with **2**. The molecular structures of **7a** and **7a′** were determined by single-crystal X-ray diffraction. The phosphorus atom is surrounded by substituents in a tetrahedral environment. A P–N single bond (1.676(3) Å) is observed in the molecular structure of **7a**. Heck reactions employing **7a**/$Pd(OAc)_2$ as catalyst system exhibited efficiency comparable to that of **8a**/$Pd(OAc)_2$.

Keywords: density functional calculations · Heck reaction · P ligands · palladium · tautomerism

Introduction

Trialkyl and triaryl phosphines (R_3P, Ar_3P) are among the most versatile and commonly employed ligands in reactions catalyzed by transition-metal complexes.[1] Recently, N-heterocyclic carbenes (NHC) have been introduced as potentially effective ligands for coupling reactions.[2] Nevertheless, these types of ligands are normally either air-/moisture-sensitive or expensive, and this significantly limits on their synthetic applications. Lately, the concept of using metal-containing phosphines, rather than the conventional organic phosphines in various phosphine-assisted catalytic reactions, has received a great deal of attention.[3] Probably the most widely used and best known metal-containing bidentate phosphine ligands are bis(diphenylphosphino)ferrocene (dppf, **1**) and its derivatives.[4] In the past few years, we have been developing another class of cobalt-containing (mono- or bidentate) phosphines, namely, **3**. Each of these compounds was prepared by reaction of dppm-bridged dicobalt complex [(μ-$PPh_2CH_2PPh_2$)$Co_2(CO)_6$] (**2**) with the corresponding alkynyl phosphine. This reaction allows straightforward access to a new class of phosphines having bulky character. Interestingly, besides the commonly observed palladium–phosphorus bonds, unusual palladium–cobalt bonds were formed during the complexation of **3** with palladium sources.[5] Therefore, the dicobalt fragment present in metal-containing phosphines **3** does not act merely as an innocent spectator, as in the conventional organic phosphine/metal catalyst system. The unique character of **3** indeed opens a new territory for the use of metal-containing phosphines as ligands in cross-coupling reactions. The roles played by

[a] C.-H. Wei, C.-E. Wu, Y.-L. Huang, Dr. R. G. Kultyshev, Prof. F.-E. Hong
Department of Chemistry
National Chung Hsing University
Taichung 40227 (Taiwan)
Fax: (+886) 4-2286-2547
E-mail: fehong@dragon.nchu.edu.tw

Supporting information for this article is available on the WWW under http://www.chemeurj.org/ or from the author.

these newly made compounds as assisting ligands in reactions catalyzed by palladium complexes were thoroughly explored.[6] In most cases, the phosphorus atoms of these ligands are electron-rich and, unfortunately, prone to oxidation. Oxidized ligands lose their coordination capabilities toward low-valent transition metals such as Pd^{II} or Pd^{0}, and this results in greatly reduced catalytic performance.

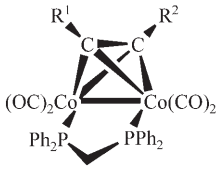

3a: R^1=PPh_2, R^2=PPh_2
3b: R^1=PPh_2, R^2=Ph
3c: R^1=PPh_2, R^2=Py
3d: R^1=PPh_2, R^2=Cy
3e: R^1=P(*t*Bu)$_2$, R^2=Ph
3f: R^1=P(*i*Pr)$_2$, R^2=Ph
3g: R^1=P(Cy)$_2$, R^2=Ph

The tautomeric equilibrium between a secondary phosphine oxide RR′HP=O (**I**) and the less stable phosphinous acid RR′POH (**I′**) is shifted to the left (Scheme 1).[7] Generally, **I′** exhibits a good coordinating capability toward low-valent transition metals, but **I** does not. Satisfactory catalytic performance for palladium-catalyzed cross-coupling reactions employing **I′**-like phosphine ligands has been reported.[8]

Scheme 1.

To the best of our knowledge, an extensive study on the tautomerism of a metal-containing phosphine oxide and the corresponding phosphinous acid has never been reported before. Therefore, we were interested in exploring the tautomerism of a metal-containing phosphine oxide using both experimental and DFT methods. Herein we report the preparation of several cobalt-containing secondary phosphine oxides and the exploration of their catalytic performance in Heck coupling reactions. In addition, results of the DFT studies on the pathways of tautomeric rearrangement available for these ligands are presented.

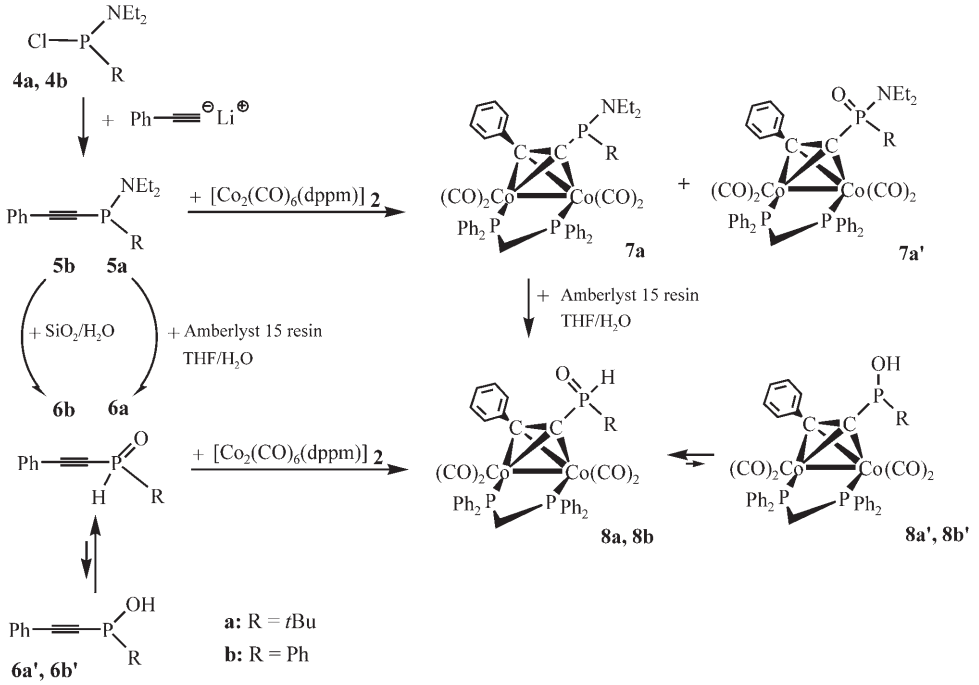

Scheme 2.

Results and Discussion

Preparation of PhC≡CP(NEt$_2$)(R) (5a: R = *t*Bu; 5b: R = Ph) and PhC≡CP(=O)(H)(R) (6a: R = *t*Bu; 6b: R = Ph): New alkynyl amino phosphine PhC≡CP(NEt$_2$)(*t*Bu) (**5a**) was prepared by a modified literature procedure (Scheme 2).[9] The ^{31}P NMR spectrum of **5a** displays a singlet at $\delta = 50.8$ ppm, which is shifted considerably upfield compared with $\delta = 161.6$ ppm for **4a**. Conversion of **5a** to secondary alkynyl phosphine oxide PhC≡CP(=O)(H)(*t*Bu) (**6a**) was achieved in acidic medium according to the ingenious preparative procedure described by Denis et al.[9] The ^{31}P NMR spectrum of **6a** displays a singlet at $\delta = 18.7$ ppm. A similar preparation was carried out for PhC≡CP(NEt$_2$)(Ph) (**5b**, Scheme 2). The ^{31}P NMR spectrum of **5b** exhibits a singlet at $\delta = 35.3$ ppm. The conversion of **5b** to PhC≡CP(=O)(H)(Ph) (**6b**) was achieved readily by column chromatography on silica.[9] In principle, a tautomeric equilibrium between **6** and the less stable secondary phosphinous acid **6′** could take place in solution (Scheme 2).

Preparation of [(μ-PPh$_2$CH$_2$PPh$_2$)Co$_2$(CO)$_4${μ,η-PhC≡CP(=O)(NEt$_2$)(R)}] (7a: R = *t*Bu; 7b: R = Ph): A bidentate ligand having both soft (e.g., P) and hard (e.g., N) donor atoms normally exhibits interesting coordinating capacity toward low-valent transition metals.[10] The relative ease of breaking/formation of the nitrogen–metal bond makes it useful in various catalytic reactions.[11] Accordingly, the coordination of P,N bidentate ligands to transition metals has recently attracted a lot of attention.[12]

Table 1. Crystal data of **7a**, **7a′**, **8a**, and **8b**.

Compound	**7a**	**7a′**	**8a**	**8b**
formula	$C_{45}H_{46}Co_2N_1O_4P_3$	$C_{45}H_{46}Co_2N_1O_5P_3$	$C_{41}H_{36}Co_2O_5P_3$	$C_{43}H_{33}Co_2O_5P_3{\cdot}CH_2Cl_2$
formula weight	875.60	891.60	822.49	925.39
cryst syst	triclinic	monoclinic	monoclinic	triclinic
space group	$P\bar{1}$	$P2(1)/n$	$P2(1)/n$	$P\bar{1}$
a [Å]	17.6981(9)	19.3785(13)	11.4373(9)	12.4124(14)
b [Å]	12.8417(6)	21.1861(14)	20.8937(17)	13.0915(15)
c [Å]	19.3480(10)	22.5262(15)	16.8703(13)	15.1746(18)
α [°]	90.0000(10)	–	–	83.627(2)
β [°]	97.7970(10)	107.9150(10)	103.473(2)	89.614(2)
γ [°]	90.0000(10)	–	–	62.164(2)
V [Å^3]	4356.6(4)	8799.8(10)	3920.5(5)	2164.2(4)
Z	2	4	4	2
ρ_{calcd} [Mg m^{-3}]	1.335	1.346	1.393	1.420
$\lambda(Mo_{K\alpha})$ [Å]	0.71073	0.71073	0.71073	0.71073
μ [mm^{-1}]	0.913	0.907	1.011	1.044
θ range [°]	1.16–26.01	1.55–26.04	1.95–26.10	1.35–26.02
observed reflections ($F>4\sigma(F)$)	16917	17302	7728	8393
no. of refined parameters	991	1009	460	509
$R1$[a] for significant reflections	0.0417	0.0393	0.0775	0.0655
$wR2$[b] for significant reflections	0.0904	0.0818	0.1937	0.1695
GoF[c]	0.904	0.888	1.149	0.952

[a] $R1=|\Sigma(|F_o|-|F_c|)/\Sigma|F_o||$. [b] $wR2=[\Sigma w(F_o^2-F_c^2)^2/\Sigma w(F_o^2)^2]^{1/2}$. [c] $GoF=[\Sigma w(F_o^2-F_c^2)^2/(N_{reflections}-N_{parameters})]^{1/2}$.

Cobalt-containing phosphine [(μ-$PPh_2CH_2PPh_2$)-$Co_2(CO)_4${μ,η-PhC≡CP(NEt_2)(*t*Bu)}] (**7a**) and its oxidation product [(μ-$PPh_2CH_2PPh_2$)$Co_2(CO)_4${μ,η-PhC≡CP(=O)-(NEt_2)(*t*Bu)}] (**7a′**) were obtained from the reaction of PhC≡CP(NEt_2)(*t*Bu) (**5a**) with **2** (Scheme 2). Presumably, the latter was formed during chromatography. Compounds **7a** and **7a′** were identified by spectroscopic means and single-crystal X-ray diffraction (Table 1). The ^{31}P NMR spectrum of **7a** displays three sets of signals at $\delta=36.7$, 37.8 (both dppm), and 86.5 ppm [P(*t*Bu)(NEt_2)]. Compared with those of **7a**, the corresponding signals of **7a′** at $\delta=34.7$, 35.3 (both dppm), and 49.7 ppm [P(=O)(*t*Bu)(NEt_2)] were observed upfield. The ORTEP diagrams of **7a** and **7a′** are depicted in Figures 1 and 2, respectively. A P–N single bond, (**7a**: 1.676(3) Å; **7a′**: 1.652(3) Å), and a P–C(*t*Bu) single bond (**7a**: 1.878(4) Å; **7a′**: 1.837(4) Å) were observed for each compound. In addition, a P=O double bond (1.484(2) Å) was observed for **7a′**. The oxidized phosphorus atom of **7a′** is located in a nearly tetrahedral surrounding. The configuration of the rest of **7a** (or **7a′**) is similar to that of its counterpart **3e**. Attempts to prepare **7b** by a similar procedure always led to the formation of [(μ-$PPh_2CH_2PPh_2$)$Co_2(CO)_4${μ,η-PhC≡CP(=O)(H)(Ph)}] (**8b**) instead. Presumably, the polarity of the Ph group of **7b** facilitates hydrolysis of **7b** to yield **8b**.

Preparation of [(μ-$PPh_2CH_2PPh_2$)$Co_2(CO)_4${μ,η-PhC≡CP-(=O)(H)(R)}] (8a: R = *t*Bu; 8b: R = Ph): By similar procedures, cobalt-containing secondary phosphine oxides [(μ-$PPh_2CH_2PPh_2$)$Co_2(CO)_4${μ,η-PhC≡CP(=O)(H)(R)}] (**8a**: R = *t*Bu; **8b**: R = Ph) were prepared by reaction of PhC≡CP(=O)(H)(R) (**6a**: R = *t*Bu; **6b**: R = Ph) with **2**. In addition, **8a** can be prepared from **7a** by a procedure analogous to that described by Denis et al. (Scheme 2).[9] Both **8a** and **8b** were identified by NMR spectroscopy and single-crystal X-ray diffraction (Table 1). The ^{31}P NMR spectrum of **8a** shows three sets of signals at $\delta=35.8$, 33.8 (br, both dppm), and 47.2 ppm (d, P(=O)(*t*Bu)(H)). The presence of a P–H

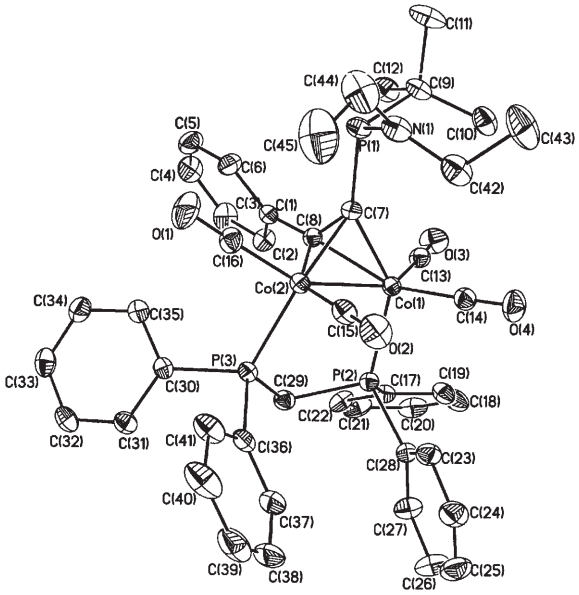

Figure 1. ORTEP drawing of **7a**. Hydrogen atoms are omitted for clarity. Selected bond lengths [Å] and angles [°]: Co(1)–C(8) 1.949(3), Co(1)–C(7) 2.002(3), Co(1)–P(2) 2.2270(9), Co(1)–Co(2) 2.4870(6), Co(2)–C(7) 1.966(3), Co(2)–C(8) 1.975(3), Co(2)–P(3) 2.2196(9), P(1)–N(1) 1.676(3), P(1)–C(7) 1.808(3), P(1)–C(9) 1.878(4), P(2)–C(29) 1.833(3), P(3)–C(29) 1.838(3), C(1)–C(8) 1.466(4), C(7)–C(8) 1.366(4); C(8)-Co(1)-C(7) 40.44(12), C(7)-Co(2)-C(8) 40.57(12), C(7)-Co(2)-Co(1) 51.83(9), N(1)-P(1)-C(7) 108.69(15), N(1)-P(1)-C(9) 105.85(17), C(7)-P(1)-C(9) 103.98(15), C(8)-C(7)-P(1) 133.6(3), Co(2)-C(7)-Co(1) 77.62(11), C(7)-C(8)-C(1) 136.0(3), Co(1)-C(8)-Co(2) 78.67(12), P(2)-C(29)-P(3) 111.84(16).

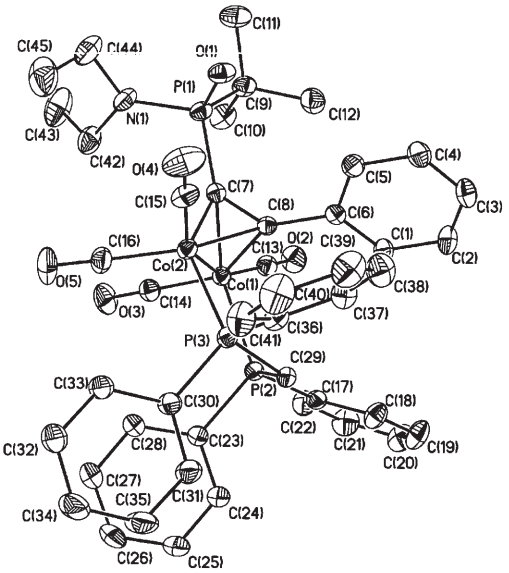

Figure 2. ORTEP drawing of **7a′**. Hydrogen atoms are omitted for clarity. Selected bond lengths [Å] and angles [°]: Co(1)−C(8) 1.951(3), Co(1)−C(7) 1.982(3), Co(1)−P(2) 2.2311(9), Co(1)−Co(2) 2.4729(6), P(1)−O(1) 1.484(2), P(1)−N(1) 1.652(3), P(1)−C(7) 1.783(3), P(1)−C(9) 1.837(4), Co(2)−C(7) 1.962(3), Co(2)−C(8) 1.979(3), Co(2)−P(3) 2.2315(9), P(2)−C(29) 1.833(3), P(3)−C(29) 1.834(3), C(6)−C(8) 1.478(4), C(7)−C(8) 1.361(4); C(8)-Co(1)-C(7) 40.48(11), O(1)-P(1)-N(1) 110.30(14), O(1)-P(1)-C(7) 110.97(13), N(1)-P(1)-C(7) 109.78(15), O(1)-P(1)-C(9) 109.89(15), N(1)-P(1)-C(9) 107.98(16), C(7)-P(1)-C(9) 107.83(15), C(42)-N(1)-C(44) 116.3(3), C(7)-Co(2)-C(8) 40.40(11), C(8)-C(7)-P(1) 132.2(2), C(7)-C(8)-C(6) 139.2(3), P(2)-C(29)-P(3) 108.44(15).

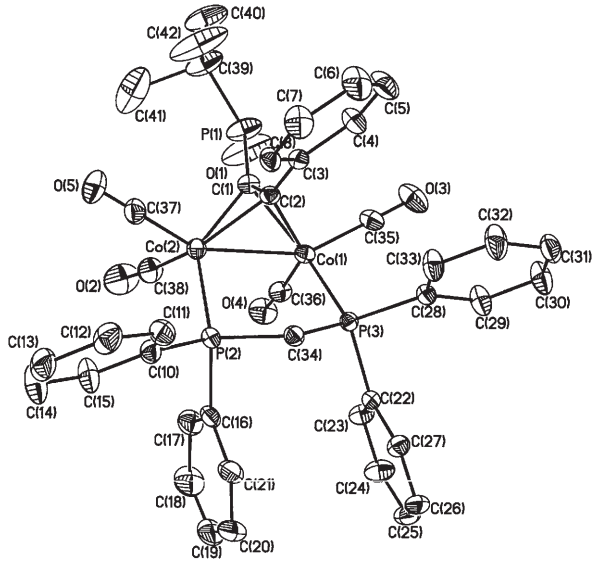

Figure 3. ORTEP drawing of **8a**. Hydrogen atoms are omitted for clarity. Selected bond lengths [Å] and angles [°]: Co(1)−C(1) 1.940(5), Co(1)−C(2) 1.981(5), Co(1)−P(3) 2.2346(13), Co(1)−Co(2) 2.4779(10), Co(2)−C(1) 1.957(5), Co(2)−C(2) 1.963(5), Co(2)−P(2) 2.2286(14), P(1)−O(1) 1.379(6), P(1)−C(39) 1.741(7), P(1)−C(1) 1.775(5), P(2)−C(34) 1.838(5), P(3)−C(34) 1.831(5), C(1)−C(2) 1.354(7), C(2)−C(3) 1.484(6); C(1)-Co(1)-C(2) 40.4(2), C(1)-Co(2)-C(2) 40.40(19), O(1)-P(1)-C(39) 122.3(4), O(1)-P(1)-C(1) 118.4(3), C(39)-P(1)-C(1) 112.9(3), C(2)-C(1)-P(1) 144.4(4), Co(1)-C(1)-Co(2) 78.96(19), C(1)-C(2)-C(3) 139.7(4), Co(2)-C(2)-Co(1) 77.86(17), P(2)-C(34)-P(3) 106.5(2).

bond in **8a** is evidenced by a large coupling constant of the last-named signal ($J_{P,H}=457.8$ Hz). Similarly, three sets of signals at $\delta=36.8$, 35.7 (br, both dppm), and 21.5 ppm (d, $J_{P,H}=483.4$ Hz, P(=O)(Ph)(H)) were observed in the ^{31}P NMR spectrum of **8b**. The ORTEP diagrams of **8a** and **8b** are depicted in Figures 3 and 4, respectively. In both compounds the oxidized phosphorus atoms are situated in almost tetrahedral environments. The P=O bond legths for **8a** and **8b** are 1.379(6) and 1.470(4) Å, respectively. In solution, a tautomeric equilibrium between secondary phosphine oxide **8** and its phosphinous acid form **8′** is expected.

Heck reactions employing cobalt-containing secondary phosphine oxides 8a and 8b: In principle, **8′** could act as a ligand toward a palladium complex. Therefore, the coordination of **8′** to palladium in basic media would yield a catalyst precursor ready for coupling reactions (Scheme 3).

Palladium-catalyzed Heck reactions of bromobenzene with styrene were carried out by employing **8a**, **8b**, and related secondary phosphine oxides as ligands (Scheme 4). In the general procedure for the catalytic reactions, a Schlenk tube was charged with 1.0 mmol of bromobenzene, 1.2 mmol of styrene, 2.0 mL of solvent, 1.4 mmol of a base, 1.0 mol% of $Pd(OAc)_2$, and 2.0 mol% of a secondary phosphine oxide ligand. The mixture was stirred at the designated reaction temperature and time. It was then worked up.

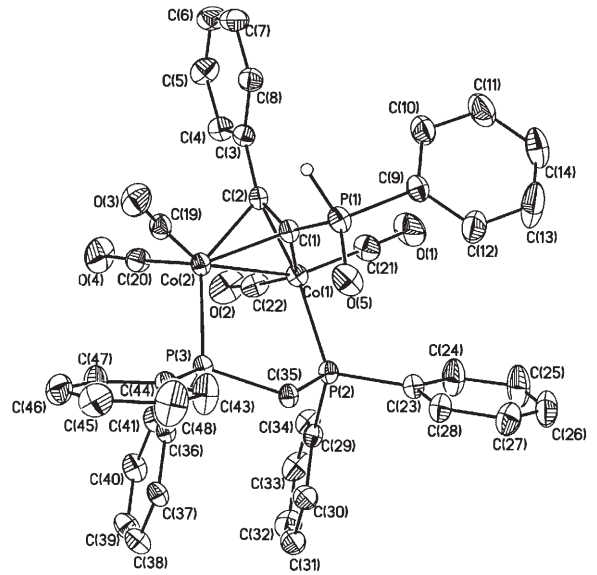

Figure 4. ORTEP drawing of **8b**. Hydrogen atoms are omitted for clarity. Selected bond lengths [Å] and angles [°]: Co(1)−C(1) 1.944(5), Co(1)−C(2) 1.965(5), Co(1)−P(2) 2.2608(16), Co(2)−C(2) 1.965(5), Co(2)−C(1) 1.968(5), Co(2)−P(3) 2.2243(15), P(1)−O(5) 1.470(4), P(1)−C(1) 1.760(5), P(1)−C(9) 1.799(6), P(2)−C(35) 1.838(5), P(3)−C(35) 1.835(5), C(1)−C(2) 1.366(7), C(2)−C(3) 1.454(7); C(1)-Co(1)-C(2) 40.9(2), P(2)-Co(1)-Co(2) 97.65(5), C(2)-Co(2)-C(1) 40.6(2), O(5)-P(1)-C(1) 116.0(2), O(5)-P(1)-C(9) 112.6(3), C(1)-P(1)-C(9) 107.3(2), C(2)-C(1)-P(1) 142.1(4), C(2)-C(1)-Co(1) 70.4(3), C(2)-C(1)-Co(2) 69.6(3), Co(1)-C(1)-Co(2) 78.96(19), C(1)-C(2)-C(3) 143.3(5), Co(2)-C(2)-Co(1) 78.5(2).

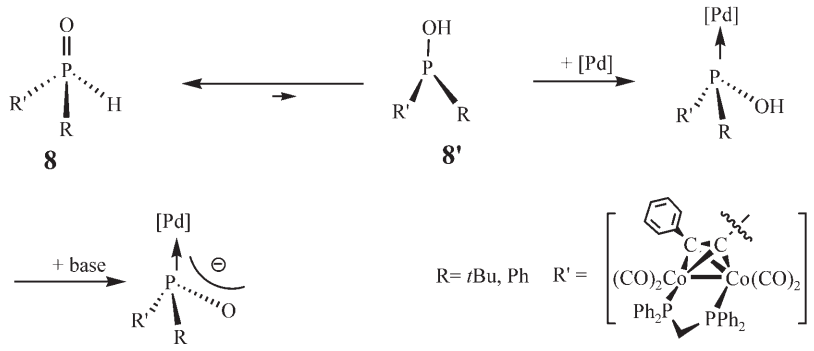

Scheme 3.

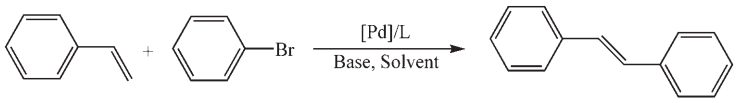

Scheme 4. Palladium-catalyzed Heck reactions with assistance by secondary phosphine oxide.

The performance of a palladium-catalyzed carbon–carbon cross-coupling reaction is governed by a number of factors.[13] Among them, a well-chosen base is crucial to the success of the reaction.[14] The influence of the base used in these coupling reactions catalyzed by secondary phosphine oxide was examined (Table 2). The best performance was observed with K_2CO_3 (Table 2, entry 1). Unexpectedly, the yield was low when a strong base such as NaO*t*Bu was employed (Table 2, entry 8).

Table 2. Heck reactions employing **8b** and various bases.[a]

Entry	Base	Yield [%][b]
1	K_2CO_3	75.1
2	KF	65.1
3	CsF	59.1
4	NEt_3	51.8
5	K_3PO_4	51.3
6	DABCO	43.8
7	Cs_2CO_3	35.5
8	NaO*t*Bu	8.5

[a] Reaction conditions: 1.0 mmol of bromobenzene, 1.2 equivalents of styrene, 1.4 equivalents of base, 2 mL DMF, 1.0 mol% of $Pd(OAc)_2$, 2.0 mol% of **8b**, 110 °C, 7 h. [b] Yield of isolated product; average of two runs.

Subsequently, the impact of various high-boiling solvents on the reaction was evaluated. As shown in Table 3, the reaction is greatly affected by the nature of the solvent used. For instance, the coupling reaction in toluene was ineffective (Table 3, entry 4). However, the yield was greatly improved when DMF was employed as solvent (Table 3, entry 1).

Carrying out the Heck reaction in DMF in the presence of K_2CO_3 at various $Pd(OAc)_2$/**8b** ratios revealed the preferred ratio (Table 4). The optimum yield was achieved with $Pd(OAc)_2$/**8b** = 1/2 (Table 4, entry 5). The positive role played by the secondary phosphine oxide ligand in the reaction can be clearly seen. Low conversion was observed in the absence of **8b** (Table 4, entry 2).

$Pd(OAc)_2$ is probably the most frequent chosen palladium source in coupling reactions due to its outstanding performance in most cases. In the following runs, the influence of various palladium sources on the reaction yield was evaluated (Table 5). Heck reactions between bromobenzene and styrene employing **8b**/**8b** and various Pd sources in the K_2CO_3/DMF system were carried out. Again, the best performance was achieved with $Pd(OAc)_2$ as palladium source (Table 5, entry 1). Interestingly, a rather

Table 3. Heck reactions employing **8b**/$Pd(OAc)_2$ or **8a**/$Pd(OAc)_2$ and K_2CO_3 as base in various solvents.[a]

Entry	Solvent	Yield [%] (L = **8b**)[b,d]	Yield [%] (L = **8a**)[c,d]
1	DMF	75.1	60.5
2	dioxane	45.6	21.6
3	DMA[e]	39.4	48.3
4	toluene	2.1	8.4

[a] Reaction conditions as in the footnote of Table 2. [b] 110 °C, 7 h. [c] 130 °C, 13 h. [d] Yield of isolated product; average of two runs. [e] DMA = *N*,*N*-dimethylacetamide.

Table 4. Dependence of the Heck reaction yield on the $Pd(OAc)_2$/**8b** ratio.[a]

Entry	Pd/L	Yield [%][b]
1	0/1	0.0
2	1/0	16.1
3	1/1	47.3
4	1/1.5	68.1
5	1/2	75.1
6	1/3	62.5
7	1.5/1	49.1
8	2/1	59.6

[a] With the exception of $Pd(OAc)_2$/**8b** ratio, reaction conditions as in the footnote of Table 2. [b] Yield of isolated product; average of two runs.

Table 5. Dependence of the Heck reaction yield on the Pd source.[a]

Entry	Pd source	Yield [%] (L = **8b**)[b,c]	Yield [%] (L = **8a**)[c,d]
1	$Pd(OAc)_2$	75.1	60.5
2	$[Pd(cod)Cl_2]$	60.5	57.6
3	$[Pd_2(dba)_3]$	59.2	49.3
4	$[Pd(CH_3CN)_2Cl_2]$	58.3	56.2
5	$[\{(\eta^3\text{-}C_3H_5)PdCl\}_2]$[e]	54.6	54.4
6	$PdCl_2$	15.7	10.7

[a] Reaction conditions as in the footnote of Table 2. [b] 110 °C, 7 h. [c] Yield of isolated product; average of two runs. [d] 130 °C, 13 h. [e] dba = *trans*,*trans*-dibenzylideneacetone.

low yield was obtained with $PdCl_2$, which is another frequently chosen palladium source (Table 5, entry 6).

Reaction temperature is another critical factor for Heck reactions. In general, Heck reactions require much high reaction temperatures than other coupling reactions. Poor performance was observed when the reaction temperature was below 110 °C (Table 6, entries 1 and 2). However, excellent yields were obtained when the reaction temperature was higher than 120 °C (Table 6, entries 5 and 6).

Table 6. Dependence of the Heck reaction yield on temperature.[a]

Entry	T [°C]	Yield [%][b]
1	90	7.8
2	100	9.2
3	110	75.1
4	120	90.1
5	130	>99.0
6	140	>99.0

[a] With the exception of temperature, reaction conditions as in the footnote of Table 2. [b] Yield of isolated product; average of two runs.

In a $Pd(OAc)_2$-catalyzed coupling reaction an induction period due to reduction of Pd^{II} to Pd^0 active species is observed.[15] This is particularly true of the Heck reaction, which requires more severe reaction conditions. A satisfactory result was obtained when the reaction was carried out at 120 °C for 5 h (Table 7, entry 3). On the contrary, the yield dropped to 68.6% or even 20.5% (Table 7, entries 2 and 1) when the reaction time was shortened to 3 or 1 h. Prolonging the reaction time might lead to the decomposition of the active catalyst and eventually diminish the reactivity. Side reactions may occur as well (Table 7, entry 4).

Table 7. Dependence of the Heck reaction yield on reaction time.[a]

Entry	Time [h]	Yield [%][b]
1	1	20.5
2	3	68.6
3	5	93.1
4	7	90.1

[a] With the exception of reaction time, reaction conditions as in the footnote of Table 2. [b] Yield of isolated product; average of two runs.

While the Heck coupling reaction with 1.0 mol% of $Pd(OAc)_2$ was effective (Table 8, entry 1), 0.1 mol% of catalyst resulted in a much poorer performance (Table 8, entry 2).

It has been commonly observed that in a palladium-catalyzed coupling reaction a better conversion is achieved with aryl halides bearing electron-withdrawing rather than electron-donating substituents.[16] Nevertheless, the reverse trend was observed in the $Pd(OAc)_2$/**8a**-catalyzed Heck reaction, where the best yields were obtained with aryl halides bearing electron-donating groups (Table 9, entries 5 and 6).[17] Poor performance was observed with *o*-bromotoluene due to severe steric hindrance (Table 9, entry 7). As expected from the generally accepted mechanism, *trans*-1,2-diarylethylene **B** rather than 1,1-diarylethylene **A** was obtained as the major product of the reaction (Scheme 5).

Table 8. Dependence of the Heck reaction yield on $Pd(OAc)_2$ concentration.[a]

Entry	[Pd] [mol%]	Yield [%][b]
1	1.0	93.1
2	0.1	51.2

[a] With the exception of temperature (120 °C), the reaction conditions as in the footnote of Table 2. [b] Yield of isolated product; average of two runs.

Table 9. Dependence of the yield of Heck reaction with $Pd(OAc)_2$/**8b** or $Pd(OAc)_2$/**8a** on substrate.[a]

		L=**8b**[b,d]		L=**8a**[c,d]	
Entry	Substrate	Yield [%]	**A**/**B**	Yield [%]	**A**/**B**
1	4-NO_2	83.6	3/97	52.4	1/99
2	4-$COCH_3$	84.4	2/98	54.1	1/99
3	4-COH	70.1	10/90	40.3	3/97
4	H	93.1	0/100	60.5	0/100
5	4-CH_3	>99.0	1/99	62.3	2/98
6	4-OCH_3	>99.0	19/81	63.7	5/95
7	2-CH_3	21.5	0/100	14.1	0/100

[a] Reaction conditions as in the footnote of Table 2. [b] 120 °C, 5 h. [c] 130 °C, 13 h. [d] Yield of isolated product; average of two runs.

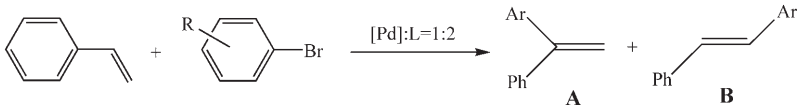

Scheme 5.

For the purpose of comparison, the same Heck reactions employing various phosphine ligands were carried out in DMF at 120 °C for 7 h. A poor yield was observed in the absence of ligand (Table 10, entry 1). The yields were greatly improved on addition of **7a**, **8b**, or **3e** (Table 10, entries 2, 4, and 5). After 7 h of reaction, almost quantitative yield was observed with **7a** as ligand (Table 10, entry 2).

Table 10. Heck reactions with various ligands.[a]

Entry	Ligand	Time [h]	Yield [%][b]	**A**/**B**
1	–	7	30.2[c]	7/93
2	**7a**	5(7)	80.6(>99.0)[c]	1/99(1/99)
3	**7a′**	7	45.7[c]	11/89
4	**8b**	5	90.1[c]	0/100
5	**3e**	5	>99.0[d]	0/100
6	**3b**	5	63.7[d]	2/98
7	**3f**	5	52.6[d]	1/99

[a] Reaction conditions as in the footnote of Table 2. [b] Yield of isolated product; average of two runs. [c] Base = K_2CO_3. [d] Base = K_3PO_4.

Table 11 shows the results obtained for Heck reactions assisted by **7a**. The trend previously observed in Table 9 is also apparent here: the catalytic performance was reduced

Table 11. Dependence of the yield of Heck reaction with **7a** as ligand on substrate.[a]

Entry	Substrate (R)	Yield [%][b]	**A/B**
1	4-NO_2	93.5	2/98
2	4-$COCH_3$	86.2	4/96
3	4-COH	75.1	8/92
4	H	>99.0	1/99
5	4-CH_3	97.1	1/99
6	4-OCH_3	>99.0	10/90
7	2-CH_3	96.8	2/98

[a] Reaction conditions as in the footnote of Table 2. The reaction was carried out in DMF at 120 °C for 7 h. [b] Yield of isolated product; average of two runs.

when electron-withdrawing groups were present in the substrate Table 11 (Table 11, entries 1–3). On the contrary, almost quantitative yields were observed with electron-donating groups (Table 11, entries 5 and 6) even in the case of *o*-bromotoluene (Table 11, entry 7). This indicates that the steric effect is much more important in the case of **8a** than in the case of **7a**.

For further comparison, the Heck reaction between bromotoluene and styrene employing in-situ-prepared $Pd(OAc)_2$/**8a** was carried out with different bases at different temperatures. Results similar to those demonstrated by the $Pd(OAc)_2$/**8b** system were obtained (Tables 12, 3, 5, and 9).

Table 12. Dependence of the yield of palladium-catalyzed Heck reaction with **8a** as ligand on base, reaction time and temperature.[a]

Entry	Base	Time [h]	*T* [°C]	Yield [%][b]
1	K_2CO_3	7	110	42.7
2	KF	7	110	33.2
3	K_3PO_4	7	110	11.9
4	CsF	7	110	trace
5	Cs_2CO_3	7	110	trace
6	K_2CO_3	5	120	29.4
7	K_2CO_3	7	120	47.8
8	K_2CO_3	7	130	59.8
9	K_2CO_3	13	130	60.5

[a] Reaction conditions as in the footnote of Table 2. [b] Yield of isolated product; average of two runs.

The best catalytic performance was obtained with $Pd(OAc)_2$/**8a** = 1/2, DMF as solvent, and K_2CO_3 as base. In general, lower efficiencies were observed than with in-situ-prepared $Pd(OAc)_2$/**8b**.

Computational studies on the tautomerism of 6 and 6′ as well as 8 and 8′: Density functional theory (DFT) has proved itself repeatedly as a useful tool in providing reliable results in studies on transition-metal-mediated catalytic reactions.[18] This method at the B3LYP level was utilized to examine the validity of the proposed routes for transformation of **8** to **8′** and that of its organic counterpart PhC≡CP(=O)(H)(*t*Bu) (**6**) to **6′** (Scheme 2). To make the computations feasible, smaller model compounds replaced the real reaction participants. Thus, the *t*Bu and Ph groups were replaced by Me and H groups, respectively.

Two probable routes for the transformation of secondary phosphine oxides to phosphinous acids were proposed and examined. The first pathway, referred to as the monomer route, is based on intramolecular hydrogen migration. The second pathway, or dimer route, is based on intermolecular hydrogen transfer.

DFT studies on the monomer route: In the monomer route, conversion of the phosphine oxide to the phosphinous acid takes place via an intramolecular hydrogen migration (Scheme 6).

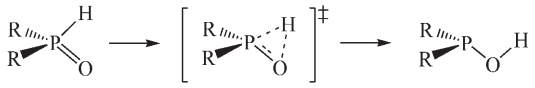

Scheme 6. Conversion of a phosphine oxide to a phosphinous acid via the monomer route (Case 1A: R = CH_3; Case 1B: R = CF_3).

In the case of the monomer route for an organic phosphine oxide, the geometry-optimized molecular structures, including the transition state, on the way from **1PO** to **1POH** (Case 1A) are shown in Figure 5. The outward appearance of **1PO** on the B3LYP potential energy surface is a distorted tetrahedron (T_d) with the phosphorus atom at its center. The configuration of **1POH** is a triangular pyramid with the phosphorus atom situated on top. On the **1PO**→**1TS**→**1POH** pathway, H1 (from P1 of **1PO**) is transferred to O1 and a new O1−H1 bond is generated. Except for H1, the relative positions of all other atoms remain almost unchanged. The O1-P1-H1 bond angle is 115.1° in **1PO**. In **1POH** the P1-O1-H1 bond angle is 108.6°. The two methyl carbon atoms, P1, and H1 are almost coplanar in **1TS**.

Similar geometry-optimized molecular structures, including the transition state on the way from **FPO** to **FPOH**,

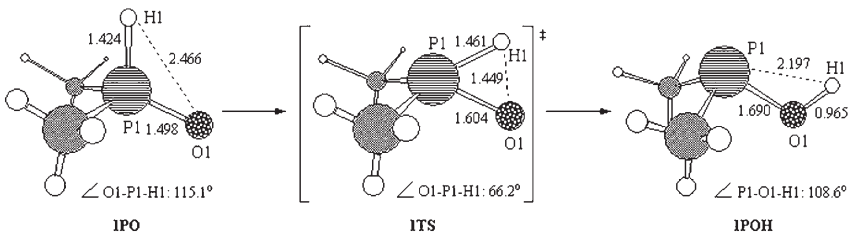

Figure 5. Optimized structures of stationary points pertinent to Case 1A showing bond lengths [Å] and angles [°].

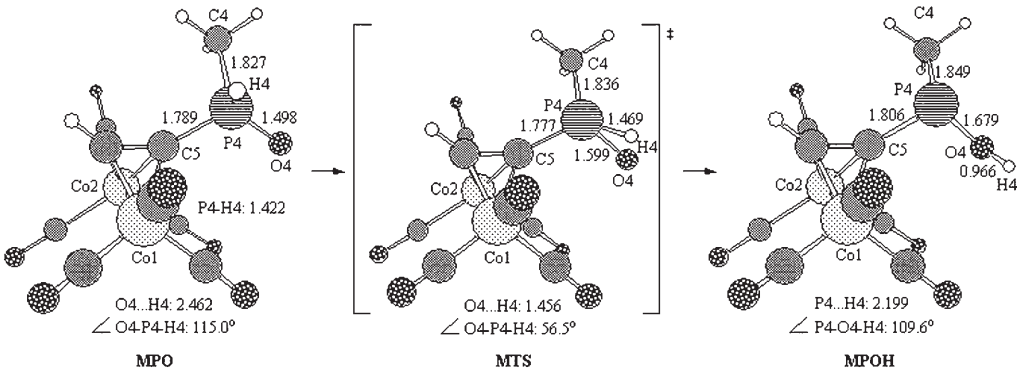

Figure 6. Optimized structures of stationary points pertinent to Case 2 showing bond lengths [Å] and angles [°].

were observed for Case 1B, where both methyl groups are replaced by CF_3 substituents.

In the case of the monomer route for a metal-containing phosphine oxide (Case 2), the geometry-optimized molecular structures, including the transition states on the way from **MPO** to **MPOH**, are shown in Figure 6. Results were similar to those obtained for Case 1. The phosphorus atom is located in the center of a distorted tetrahedron in **MPO** on the B3LYP potential energy surface. An analogous triangular pyramid was observed for **MPOH** with the phosphorus atom located at the top. On the **MPO**→**MTS**→**MPOH** pathway, H4 (from P4 of **MPO**) is transferred to O4 of **4POH** with creation of a new O4–H4 bond. The O4-P4-H4 bond angle is 115.0° in **MPO**. In **MPOH**, the P4-O4-H4 bond angle is 109.6°. There is little geometric change on the side of the metal moiety during the conversion.

DFT studies on the dimer route: As shown in Scheme 7, the transformation of phosphine oxide into phosphinous acid is possible via intermolecular hydrogen transfer.

In the case of the dimer route for an organic phosphine oxide (Case 3), the geometry-optimized molecular structures, including transition states on the way from **2PO** to **2POH**, are depicted in Figure 7. First, two phosphine oxide molecules approach each other and adopt the proper orientation. Then, two hydrogen atoms are transferred synchronously to the oxygen atoms of the opposite molecules. Finally, the two phosphinous acid molecules formed move away from each other. In **2PO** six atoms, H2, P2, O2, H3, P3, O3, are arranged in a chair form. They lie almost in the same plane in **2TS** and **2POH**.

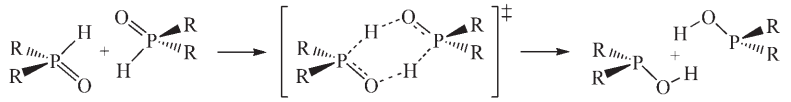

Scheme 7. Conversion of a phosphine oxide to a phosphinous acid via the dimer route (R = CH_3)

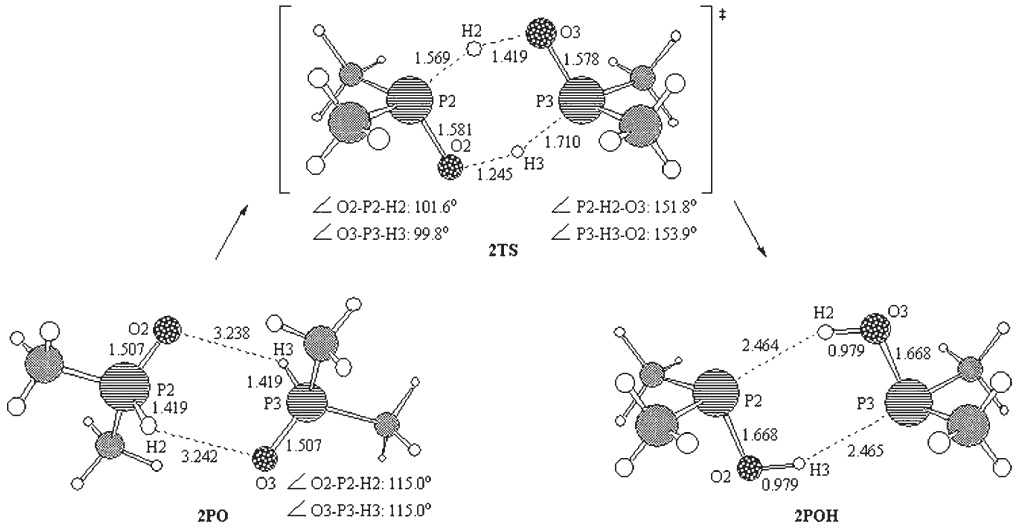

Figure 7. Optimized structures of stationary points pertinent to Case 3 showing bond lengths [Å] and angles [°].

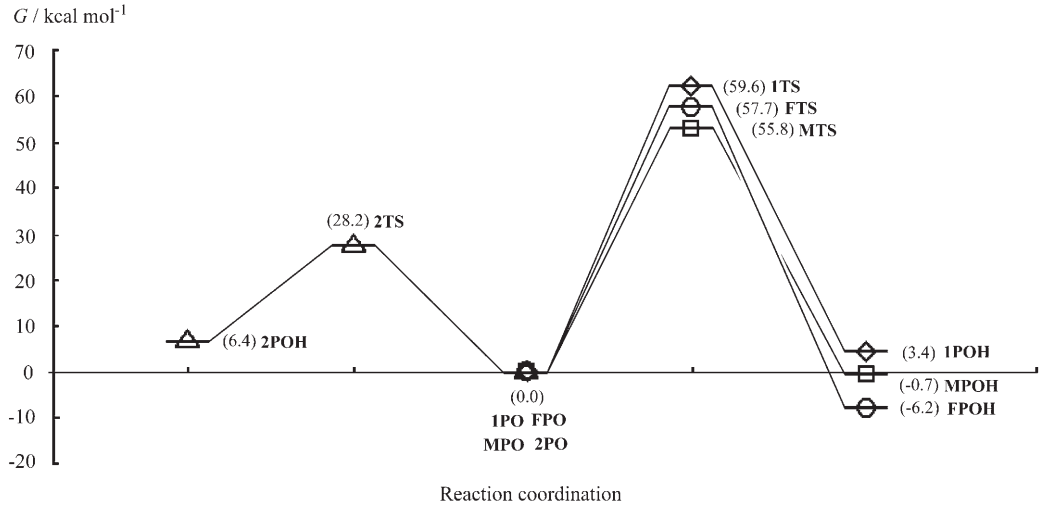

Figure 8. Free energies showing bond lengths [Å] and angles [kcal mol^{-1}] of states involved in Case 1 A (diamond), Case 1 B (circle), Case 2 (square), and Case 3 (triangle), calculated at the B3LYP level of theory.

The potential energy surfaces of the proposed transformations of Cases 1 A, 1 B, 2, and 3 are depicted in Figure 8. First, in the intramolecular transfer process the activation energy for the metal-containing species is lower than that for its organic counterpart. It is 55.8 kcal mol^{-1} for Case 2 versus 59.6 kcal mol^{-1} and 57.7 kcal mol^{-1} for Case 1 A and Case 1 B, respectively. Obviously, the presence of the metal fragment assists in lowering the activation energy. The replacement of CH_3 groups by the strongly electron-withdrawing CF_3 groups also reduces the activation energy. Bis(trifluoromethyl)phosphinous acid is also more stable than the corresponding phosphine oxide and dimethylphosphinous acid. In fact, it has been shown experimentally that bis(trifluoromethyl)phosphinous acid is not prone to rearrange to the oxide.[19] Second, the activation energy is significantly lower for the intermolecular hydrogen transfer process (Case 3). The severe strain caused by formation of a three-membered ring during the intramolecular hydrogen migration processes (Cases 1 and 2) is avoided in the intermolecular processes (Case 3).

It has been shown that in the monomer route the transformation of the transition metal-containing compound proceeds with a lower activation energy. It has also been demonstrated that the conversion via the dimer route is much more feasible than that via the monomer route. However, due to the severe steric hindrance caused by the bulkiness of the metal-containing compound, the dimer route is probably not feasible for a compound with a bulky substituent, such as **8a**.[20] Therefore, the **8a**→**8a′** conversion is less likely. However, our experimental observation that **8b** is an efficient ligand in the Pd-catalyzed Heck reaction between bromobenzene and styrene suggests that the transformation **8b**→**8b′** indeed occurs to some extent in solution.

Summary

We have demonstrated that novel cobalt-containing secondary phosphine oxides **8a** and **8b** could be prepared by the reactions of corresponding secondary phosphine oxides **6a** and **6b** with dppm-bridged dicobalt complex **2**. Using **8a** as ligand in palladium-catalyzed Heck reactions led to poor results, probably due to the extremely low quantity of its tautomeric form **8a′** in solution. Nevertheless, reactions employing **8b** under the same conditions are very efficient. Density functional calculations on the transformation **8**→**8′** supports the experimental results. The dimer route has been shown to have a much lower activation energy than the monomer route for the transformation **8**→**8′**. In the dimer route, two reacting molecules must approach each other and arrange themselves in the proper orientation. Since the *t*Bu group of **8a** is much larger than the Ph group of **8b**, it is much more difficult for two **8a** molecules to engage appropriately. Therefore, the catalytic reaction relying on the transformation **8a**→**8a′** is much less effective.

Experimental Section

General information: All manipulations were carried out under a dry nitrogen atmosphere. Solvents and deuterated solvents were purified before use. Products were mostly separated by centrifugal thin layer chromatography (CTLC, Chromatotron, Harrison model 8924). The ^{1}H and ^{31}P NMR spectra were recorded on a Varian-400 spectrometer at 400.44 and 162.10 MHz, respectively; ^{13}C NMR spectra were recorded on a Varian VXR-300S spectrometer at 75.43 MHz. Chemical shifts are reported in parts per million relative to the residual proton signals of $CDCl_3$ or CD_2Cl_2. Mass spectra were recorded on a JOEL JMS-SX/SX 102 A GC/MS/MS spectrometer. Elemental analyses were obtained on a Heraeus CHN-O-S-Rapid instrument.

7a and 7a′: A solution of $[Co_2(CO)_6(dppm)]$ (**2**, 1.340 g, 2.000 mmol) and PhC≡CP(*t*Bu)(NEt_2) (**5a**, 0.523 g, 2.000 mmol) in THF (15 mL) was stirred at 70 °C for 16 h. Then the solvent was removed under reduced pres-

sure, and the resulting dark red residue was separated by CTLC. A dark red band was eluted with hexanes/CH_2Cl_2 (1:1). The product was identified as **7a** (1.365 g, 1.560 mmol, 78.0% yield). A similar procedure was used for the preparation of **7a′**: A solution of $[Co_2(CO)_6(dppm)]$ (**2**, 1.340 g, 2.000 mmol) and PhC≡CP(=O)(*t*Bu)(NEt_2) (0.555 g, 2.000 mmol) in THF (15 mL) was stirred at 70 °C for 16 h and then worked up. A dark red band was eluted with ethyl acetate/CH_2Cl_2 (1:1). The product was identified as **7a′** (1.568 g, 1.760 mmol, 88.0% yield).

7a: ^{1}H NMR ($CDCl_3$): $\delta = 7.39–6.75$ (m, 24H; arene), 3.48 (m, 1H; dppm), 3.27 (m, 4H; NEt_2), 3.11 (m, 1H; dppm), 1.45 (t, 6H; NEt_2), 1.10–1.19 ppm (d, 9H; P*t*Bu); ^{13}C NMR ($CDCl_3$, δ/ppm): 133.07–127.86 (arene), 30.43 (dppm); ^{31}P NMR ($CDCl_3$, δ/ppm): 37.80–36.72 (d, dppm), 86.52 ppm (s, $PNEt_2$); MS (FAB): *m*/*z*: 876.5 $[M+1]^+$; elemental analysis (%) calcd for **7a**: N 1.60, C 61.71, H 5.26; found: N 1.11, C 61.20, H 54.88.

7a′: ^{1}H NMR ($CDCl_3$): $\delta = 7.81–6.71$ (m, 24H; arene), 3.25 (m, 1H; dppm), 3.41 (m, 1H; dppm), 2.72 (m, 4H; NEt_2), 1.69 (t, 6H; NEt_2), 1.15 ppm (d, 9H; P*t*Bu); ^{13}C NMR ($CDCl_3$): $\delta = 133.07–127.86$ (arene), 30.43 ppm (dppm); ^{31}P NMR ($CDCl_3$): $\delta = 49.28$ (s, P(=O)(NEt_2)), 35.27 ppm (d, dppm); MS (FAB): *m*/*z*: 892.6 $[M+1]^+$; elemental analysis (%) calcd for **7a′**: N 1.57, C 60.51, H 5.16; found: N 1.31, C 59.51, H 5.23.

8a and 8b: A solution of PhC≡CP(=O)(H)(*t*Bu) (**6a**, 0.412 g, 2.000 mmol) in THF (5 mL) was added to $[Co_2(CO)_6(dppm)]$ (**2**, 1.340 g, 2.000 mmol) and THF (10 mL). The mixture was stirred for 24 h at room temperature. The solvent was removed under reduced pressure, and the resulting dark red residue purified by CTLC. A dark red band was eluted with CH_2Cl_2/ethyl acetate (10:1). It was identified as **8a** (1.246 g, 1.520 mmol, 76.0% yield). A similar procedure was used for the preparation of **8b**: A solution of $[Co_2(CO)_6(dppm)]$ (**2**, 1.340 g, 2.000 mmol) and PhC≡CP(Ph)(NEt_2) (**6b**, 0.563 g, 2.000 mmol) in THF (15 mL) was stirred at 50 °C for 8 h and then worked up. The solvent was removed under reduced pressure, and the resulting dark red residue was purified by CTLC. A dark red band was eluted with ethyl acetate/CH_2Cl_2 (1:1). The product was identified as **8b** (1.546 g, 1.840 mmol, 92.0% yield). Apparently, the phosphorus atom was oxidized during the chromatographic process.

8a: ^{1}H NMR ($CDCl_3$): $\delta = 7.42–7.01$ (m, 25H; arene), 7.32 (d, $^1J_{PH} = 457.8$ Hz, 1H; PH), 3.33 (m, 1H; dppm), 3.00 (m, 1H; dppm), 0.883 ppm (br, 9H; *t*Bu); ^{31}P NMR ($CDCl_3$): $\delta = 47.2$ ($^1J_{PH} = 457.8$ Hz, 1P, P(=O)-(*t*Bu)(H)) 35.8 (d, 1P, dppm), 33.8 ppm (d, 1P, dppm); MS (FAB): *m*/*z*: 821.4 $[M+1]^+$; elemental analysis (%) calcd for **8a**: C 60.09, H 4.56; found: C 60.23, H 4.06.

8b: ^{1}H NMR ($CDCl_3$): $\delta = 8.92$ (d, $^1J_{PH} = 483.4$ Hz, 1H; PH), 7.69–6.98 (m, 29H; arene), 4.12 (m, 1H; dppm), 3.29 ppm (m, 1H; dppm); ^{13}C NMR ($CDCl_3$): $\delta = 133.07–127.86$ (arene), 30.43 ppm (dppm); ^{31}P NMR ($CDCl_3$): $\delta = 36.8$ (d, 1P; dppm), 35.7 (d, 1P; dppm), 21.5 ppm ($^1J_{PH} = 483.4$ Hz, 1P; P(=O)(Ph)(H)); MS (FAB): *m*/*z*: 841.4 $[M+1]^+$; elemental analysis (%) calcd for **8b**: C 61.43, H 3.93; found: C 60.82, H 3.41.

X-ray crystallographic studies: Suitable crystals of **7a**, **7a′**, **8a**, and **8b** were sealed in thin-walled glass capillaries under nitrogen atmosphere and mounted on a Bruker AXS SMART 1000 diffractometer. Intensity data were collected in 1350 frames with increasing ω (width of 0.3° per frame). The absorption correction was based on symmetry-equivalent reflections using the SADABS program. The space group determination was based on a check of the Laue symmetry and systematic absences, and was confirmed by means of the structure solution. The structure was solved by direct methods using a SHELXTL package.[21] All non-H atoms were located from successive Fourier maps and hydrogen atoms were refined by using a riding model. Anisotropic thermal parameters were used for all non-H atoms, and fixed isotropic parameters were used for H atoms.[22] Crystallographic data of **7a**, **7a′**, **8a**, and **8b** are summarized in Table 1.

CCDC-615123 (**7a**), CCDC-296107 (**7a′**), CCDC-615124 (**8a**) and CCDC-615125 (**8b**) contain the supplementary crystallographic data for this paper. These data can be obtained free of charge from the Cambridge Crystallographic Data Centre via www.ccdc.cam.ac.uk/data_request/cif.

Computational methods: All calculations were carried out using the Gaussian 03 package[23] with the tight criterion (10^{-8} Hartree) as default for the SCF convergence. The molecular geometries were fully optimized with the hybrid B3LYP-DFT method under C_1 symmetry with the Becke three-parameter exchange functional[24] and the Lee–Yang–Parr correlation functional.[25] LANL2DZ including the double-ζ basis sets for the valence and outermost core orbitals combined with pseudopotential was used for Co,[26,27] and 6-31G(d,p) basis sets were employed for the other atoms, which has proven successful in describing the cobalt-mediated Pauson–Khand reaction.[28] All the stationary points found were characterized via harmonic vibrational frequency analysis as minima (number of imaginary frequencies $N_{imag} = 0$) and transition states ($N_{imag} = 1$). For the determination of transition-state geometry, intrinsic reaction coordinate (IRC)[29] analyses followed geometry optimization to ensure the transition structures are smoothly connected by two proximal minima along the reaction coordinate. Thermodynamic quantities, calculated electronic energies, enthalpies of reaction ΔH_R, and free activation energies $\Delta G^{\neq}$, were obtained and corrected at constant pressure and 298 K. Stability analysis[30] was performed to determine whwether the Kohn–Sham (KS) solutions are stable with respect to variations which break spin and spatial symmetry. Tables listing coordinates and energies of the optimized stationary points are available as Supporting Information

Acknowledgements

We thank the National Science Council of the R.O.C. (Grant NSC 94-2113M-005-011) for financial support.

[1] a) J. Hassan, M. Sévingnon, C. Gozzi, E. Schulz, M. Lemaire, *Chem. Rev.* **2002**, *102*, 1359–1469; b) W. Tang, X. Zhang, *Chem. Rev.* **2003**, *103*, 3029–3070; c) N. G. Andersen, B. A. Keay, *Chem. Rev.* **2001**, *101*, 997–1030; d) C. A. Bessel, P. Aggarwal, A. C. Marschilok, K. J. Takeuchi, *Chem. Rev.* **2001**, *101*, 1031–1066; e) T. E. Barder, S. D. Walker, J. R. Martinelli, S. L. Buchwald, *J. Am. Chem. Soc.* **2005**, *127*, 4685–4696; f) S. D. Walker, T. E. Barder, J. R. Martinelli, S. L. Buchwald, *Angew. Chem.* **2004**, *116*, 1907–1912; *Angew. Chem. Int. Ed.* **2004**, *43*, 1871–1876; g) J. F. Hartwig, *Angew. Chem.* **1998**, *110*, 2154–2177; *Angew. Chem. Int. Ed.* **1998**, *37*, 2046–2067; h) G. Mann, J. F. Hartwig, *J. Am. Chem. Soc.* **1996**, *118*, 13109–13110; i) N. Kataoka, Q. Shelby, J. P. Stambuli, J. F. Hartwig, *J. Org. Chem.* **2002**, *67*, 5553–5566; j) A. F. Littke, C. Dai, G. C. Fu, *J. Am. Chem. Soc.* **2000**, *122*, 4020–4028; k) J. G. Planas, J. A. Gladysz, *Inorg. Chem.* **2002**, *41*, 6947–6949; l) Q.-S. Hu, Y. Lu, Z.-Y. Tang, H.-B. Yu, *J. Am. Chem. Soc.* **2003**, *125*, 2856–2857; m) T. E. Pickett, F. X. Roca, C. J. Richards, *J. Org. Chem.* **2003**, *68*, 2592–2599; n) Z.-Y. Tang, Y. Lu, Q.-S. Hu, *Org. Lett.* **2003**, *5*, 297–300.

[2] a) O. Navarro, R. A. Kelly III, S. P. Nolan, *J. Am. Chem. Soc.* **2003**, *125*, 16194–16195; b) M. S. Viciu, R. A. Kelly III, E. D. Stevens, F. Naud, M. Studer, S. P. Nolan, *Org. Lett.* **2003**, *5*, 1479–1482; c) J. Yin, M. P. Rainka, X. X. Zhang, S. L. Buchwald, *J. Am. Chem. Soc.* **2002**, *124*, 1162–1163; d) J. P. Stambuli, R. Kuwano, J. F. Hartwig, *Angew. Chem.* **2002**, *114*, 4940–4942; *Angew. Chem. Int. Ed.* **2002**, *41*, 4746–4748.

[3] a) S. Eichenseher, O. Delacroix, K. Kromm, F. Hampel, J. A. Gladysz, *Organometallics* **2005**, *24*, 245–255; b) O. Delacroix, J. A. Gladysz, *Chem. Commun.* **2003**, 665–675; c) K. Kromm, F. Hampel, J. A. Gladysz, *Organometallics* **2002**, *21*, 4264–4274.

[4] a) T. J. Colacot, *Chem. Rev.* **2003**, *103*, 3101–3118; b) R. C. J. Atkinson, V. C. Gibson, N. J. Long, *Chem. Soc. Rev.* **2004**, *33*, 313–328.

[5] F.-E Hong, C.-P. Chang, Y.-C. Chang, *Dalton Trans.* **2003**, 3892–3897.

[6] a) F.-E Hong, Y.-C. Chang, R.-E Chang, S.-C. Chen, B.-T. Ko, *Organometallics* **2002**, *21*, 961–967; b) F.-E Hong, C.-P. Chang, Y.-C. Chang, *Dalton Trans.* **2003**, 3892–3897; c) F.-E Hong, Y.-C. Lai, Y.-J.

Ho, Y.-C. Chang, *J. Organomet. Chem.* **2003**, *688*, 161–167; d) F.-E Hong, Y.-C. Chang, C.-P. Chang, Y.-L. Huang, *Dalton Trans.* **2004**, 157–165; e) F.-E Hong, Y.-J. Ho, Y.-C. Chang, Y.-C. Lai, *Tetrahedron* **2004**, *60*, 2639–2645; f) F.-E Hong, Y.-J. Ho, Y.-C. Chang, Y.-L. Huang, *J. Organomet. Chem.* **2005**, *690*, 1249–1257; g) C.-P. Chang, Y.-L. Huang, F.-E Hong, *Tetrahedron* **2005**, *61*, 3835–3839; h) J.-C. Lee, M.-G. Wang, F.-E Hong, *Eur. J. Inorg. Chem.* **2005**, 5011–5017; i) Y.-C. Chang, F.-E Hong, *Organometallics* **2005**, *24*, 5686–5695.

[7] a) K. R. Dixon, A. D. Rattray, *Can. J. Chem.* **1971**, *49*, 3997–4004; b) G. O. Doak, L. D. Freedman, *Chem. Rev.* **1961**, *61*, 31–44; c) B. Silver, Z. Luz, *J. Am. Chem. Soc.* **1962**, *84*, 1091–1905; d) Z. Luz, B. Silver, *J. Am. Chem. Soc.* **1961**, *83*, 4518–4521; e) Z. Luz, B. Silver, *J. Am. Chem. Soc.* **1962**, *84*, 1095–1098.

[8] a) G. Y. Li, *Angew. Chem.* **2001**, *113*, 1561–1564; *Angew. Chem. Int. Ed.* **2001**, *40*, 1513–1516; b) G. Y. Li, G. Zheng, A. F. Noonan, *J. Org. Chem.* **2001**, *66*, 8677–8681; c) L. Ackermann, R. Born, J. H. Spatz, D. Meyer, *Angew. Chem.* **2005**, *117*, 7382–7386; *Angew. Chem. Int. Ed.* **2005**, *44*, 7216–7219; d) L. Ackermann, R. Born, *Angew. Chem.* **2005**, *117*, 2497–2500; *Angew. Chem. Int. Ed.* **2005**, *44*, 2444–2447; e) I. Pryjomska, H. B. Bechowski, Z. Ciunik, A. M. Trzeciak, J. J. Ziółkowski, *Dalton Trans.* **2006**, 213–220.

[9] a) G. Baba, J.-F. Pilard, K. Tantaoul, A.-C. Gaumont, J.-M. Denis, *Tetrahedron Lett.* **1995**, *36*, 4421–4424; b) J.-F. Pilard, G. Baba, A.-C. Gaumont, J.-M. Denis, *Synlet* **1995**, 1168–1170.

[10] a) R. G. Pearson, *J. Am. Chem. Soc.* **1963**, *85*, 3533–3539; b) *Hard and Soft Acids and Bases* (Ed.: R. G. Pearson), Dowden, Hutchinson, and Ross, Stroudsburg, PA, **1973**; c) R. G. Pearson, *Chemical hardness - A historical introduction, Struct. Bonding (Berlin)* **1993**, *80*, 1–10.

[11] a) J. P. Farr, M. M. Olmstead, F. E. Wood, A. L. Balch, *J. Am. Chem. Soc.* **1983**, *105*, 792–798; b) E. Linder, H. Rauleder, P. Wegner, *Z. Naturforsch. B* **1984**, *39*, 1224–1229; c) K. Kurtev, D. Ribola, R. A. Jones, D. J. Cole-Hamilton, G. Wilkinson, *J. Chem. Soc. Dalton Trans.* **1980**, 55–58.

[12] a) Z.-Z Zhang, H. Cheng, *Coord. Chem. Rev.* **1996**, *147*, 1–39; b) Z.-Z. Zhang, H.-K. Wang, Z. Xi, X.-K. Yao, R.-J. Wang, *J. Organomet. Chem.* **1989**, *376*, 123–131; c) Z.-Z. Zhang, H.-K. Wang, H.-G. Wang, R.-J. Wang, *J. Organomet. Chem.* **1986**, *314*, 357–367; d) J. P. Farr, M. M. Olmstead, N. M. Rutherford, F. E. Wood, A. L. Balch, *Organometallics* **1983**, *2*, 1758–1762; e) J. P. Farr, F. E. Wood, A. L. Balch, *Inorg. Chem.* **1983**, *22*, 1229–1235; f) J. P. Farr, M. M. Olmstead, A. L. Balch, *Inorg. Chem.* **1983**, *22*, 3387–3393; g) R. J. Puddephatt, *Chem. Soc. Rev.* **1983**, *12*, 99–127.

[13] a) E. R. Goldman, I. L. Medintz, J. L. Whitley, A. Hayhurst, A. R. Clapp, H. T. Uyeda, J. R. Deschamps, M. E. Lassman, H. Mattoussi, *J. Am. Chem. Soc.* **2005**, *127*, 6744–6751; b) A. A. C. Braga, N. H. Morgon, G. Ujaque, F. Maseras, *J. Am. Chem. Soc.* **2005**, *127*, 9298–9307.

[14] a) N. Miyaura, K. Yamada, H. Suginome, A. Suzuki, *J. Am. Chem. Soc.* **1985**, *107*, 972–980; b) G. A. Grasa, A. C. Hillier, S. P. Nolan, *Org. Lett.* **2001**, *3*, 1077–1080; c) S. R. Dubbaka, P. Vogel, *Org. Lett.* **2004**, *6*, 95–98.

[15] a) R. F. Heck, J. P. Nolley, Jr., *J. Org. Chem.* **1972**, *37*, 2320–2322; b) I. P. Beletskaya, A. V. Cheprakov, *Chem. Rev.* **2000**, *100*, 3009–3066; c) Q. Yao, E. P. Kinney, Z. Yang, *J. Org. Chem.* **2003**, *68*, 7528–7531; d) J. Mo, L. Xu, J. Xiao, *J. Am. Chem. Soc.* **2005**, *127*, 751–760; e) P. Fristrup, S. L. Quement, D. Tanner, P.-O. Norrby, *Organometallics* **2004**, *23*, 6160–6165.

[16] N. Kataoka, Q. Shelby, J. P. Stambuli, J. F. Hartwig, *J. Org. Chem.* **2002**, *67*, 5553–5566.

[17] a) Z. Xiong, N. Wang, M. Dai, A. Li, J. Chen, Z. Yang, *Org. Lett.* **2004**, *6*, 95–98; b) R. Singh, M. S. Viciu, N. Kramareva, O. Navarro, S. P. Nolan, *Org. Lett.* **2005**, *7*, 1829–1832; c) C. Dai, G. C. Fu, *J. Am. Chem. Soc.* **2001**, *123*, 2719–2724; d) M. E. Limmert, A. H. Roy, J. F. Hartwig, *J. Org. Chem.* **2005**, *70*, 9364–9370.

[18] a) J. A. Pople, *Angew. Chem.* **1999**, *111*, 2014–2023; *Angew. Chem. Int. Ed.* **1999**, *38*, 1894–1902; b) W. J. Hehre, L. Radom, P. von R. Schleyer, J. A. Pople, *Ab Initio Molecular Orbital Theory*, Wiley-Interscience, New York, **1986**; c) W. Koch, M. C. Holthausen, *A Chemist's Guide to Density Functional Theory*, Wiley-VCH, Weinheim, **2000**; d) T. Ziegler, *Chem. Rev.* **1991**, *91*, 651–667; e) E. R. Davidson, *Chem. Rev.* **2002**, *102*, 351–352.

[19] J. E. Griffiths, A. B. Burg, *J. Am. Chem. Soc.* **1962**, *84*, 3442–3450.

[20] D. G. Ho, R. Gao, J. Celaje, H.-Y. Chung, M. Selke, *Science* **2003**, *302*, 259–262.

[21] G. M. Sheldrick, SHELXTL PLUS User's Manual, Revision 4.1, Nicolet XRD Corporation, Madison, Wisconsin, **1991**.

[22] The hydrogen atoms rode on carbon or oxygen atoms in their idealized positions and were held fixed with C–H distances of 0.96 Å.

[23] Gaussian 03, Revision C.02, M. J. Frisch, G. W. Trucks, H. B. Schlegel, G. E. Scuseria, M. A. Robb, J. R. Cheeseman, J. A. Montgomery, Jr., T. Vreven, K. N. Kudin, J. C. Burant, J. M. Millam, S. S. Iyengar, J. Tomasi, V. Barone, B. Mennucci, M. Cossi, G. Scalmani, N. Rega, G. A. Petersson, H. Nakatsuji, M. Hada, M. Ehara, K. Toyota, R. Fukuda, J. Hasegawa, M. Ishida, T. Nakajima, Y. Honda, O. Kitao, H. Nakai, M. Klene, X. Li, J. E. Knox, H. P. Hratchian, J. B. Cross, C. Adamo, J. Jaramillo, R. Gomperts, R. E. Stratmann, O. Yazyev, A. J. Austin, R. Cammi, C. Pomelli, J. W. Ochterski, P. Y. Ayala, K. Morokuma, G. A. Voth, P. Salvador, J. J. Dannenberg, V. G. Zakrzewski, S. Dapprich, A. D. Daniels, M. C. Strain, O. Farkas, D. K. Malick, A. D. Rabuck, K. Raghavachari, J. B. Foresman, J. V. Ortiz, Q. Cui, A. G. Baboul, S. Clifford, J. Cioslowski, B. B. Stefanov, G. Liu, A. Liashenko, P. Piskorz, I. Komaromi, R. L. Martin, D. J. Fox, T. Keith, M. A. Al-Laham, C. Y. Peng, A. Nanayakkara, M. Challacombe, P. M. W. Gill, B. Johnson, W. Chen, M. W. Wong, C. Gonzalez, and J. A. Pople, Gaussian, Inc., Wallingford, CT, **2004**.

[24] A. D. Becke, *J. Chem. Phys.* **1993**, *98*, 5648–5652.

[25] C. Lee, W. Yang, R. G. Parr, *Phys. Rev. B* **1988**, *37*, 785–789.

[26] T. H. Dunning, Jr., P. J. Hay, *Modern Theoretical Chemistry*, Plenum, New York, **1976**, p. 1.

[27] P. J. Hay, W. R. Wadt, *J. Chem. Phys.* **1985**, *82*, 299–310.

[28] M. Yamanaka, E. Nakamura, *J. Am. Chem. Soc.* **2001**, *123*, 1703–1708.

[29] a) C. Gonzalez, H. B. Schlegel, *J. Chem. Phys.* **1989**, *90*, 2154–2161; b) C. Gonzalez, H. B. Schlegel, *J. Phys. Chem.* **1990**, *94*, 5523–5527.

[30] a) R. Seeger, J. A. Pople, *J. Chem. Phys.* **1977**, *66*, 3045–3050; b) R. Bauernschmitt, R. Ahlrichs, *J. Chem. Phys.* **1996**, *104*, 9047–9052.

Received: July 20, 2006
Published online: November 8, 2006

